Volume 38 No. 2s, 2025

ISSN: 1311-1728 (printed version); ISSN: 1314-8060 (on-line version)

ENHANCED BRAIN TUMOR SEGMENTATION WITH SKIP CONNECTED RESNET-18 ENCODER-DECODER FRAME WORK WITH DICE LOSS

R. Lakshmi Pravallika¹, R. Pradeep Kumar Reddy^{2*}

¹Research Scholar, Department of CSE, Y.S.R.Engineering College of YVU, India

²Associate Professor, Department of CSE, Y.S.R.Engineering College of YVU, India

E-mail: ¹pravallikareddy.nl@gmail.com, ²pradeepmadhavi@gmail.com*

Abstract

The research develops an advanced brain tumor segmentation system that combines a skip connection between ResNet-18 and Dice Loss in an encoder-decoder network. Brain tumor segmentation helps medical imaging specialists find and plan better treatment methods for patients. The proposed method uses ResNet-18 as a base which combines deep architecture with residual connections to prevent vanishing gradient problems. In the technique the model connects the encoder and decoder to keep spatial details that disappear in typical architectures during down sampling steps. The method can better identify hard-to-sector tumor areas because it handles small and nonuniform tissue elements effectively. The model uses Dice Loss as its optimization method to measure how well the predicted tumor outlines match the actual tumor areas. The proposed network proves better tumor segmentation results on its regular brain data collection through testing against older technique approaches. The new model outperforms U-Net by 0.87% in accuracy plus 46.99% in precision along with better F1 scores and Dice coefficients but demonstrates an 0.84% drop in recall. The new method proves better than U-Net by revealing improved performance and segmentation outcomes. The network design efficiently segments challenging areas using its encoder-decoder structure based on ResNet-18 and Dice Loss calculations.

Key words: Brain Tumor, Dice Loss, Encoder-Decoder block, Segmentation, Skip connection, ResNet-18.

1. Introuduction

Research into brain tumors has brought major changes to medical practices in diagnosis, treatment, and patient services [1]. Medical research now uses MRI and CT scans plus AI system segmentation tools to identify brain tumors before they become severe. The field of molecular biology enables doctors to create personal treatment options based on genetic mutations which increases treatment results. Modern surgery with modern technique, including minimally invasive techniques and neuro navigation systems, make doctors more precise and

Volume 38 No. 2s, 2025

ISSN: 1311-1728 (printed version); ISSN: 1314-8060 (on-line version)

give the patients less prolonged recovery time. The introduction of techniques like stereotactic radiosurgery and proton therapy in radiation treatment has allowed for precise tumor targeting with minimal harm to healthy tissues.

The blood-brain barrier has also improved in terms of crossing. And the immunotherapy is also developing new promising treatment options by harnessing immune system to fight against tumor. The advancements achieved in these areas have enabled enhanced interdisciplinary approach in neurology, oncology as well as radiology towards initiating a more reliable prognosis, survival forecast and treatment of brain tumors in more comprehensible manners with an optimistic outlook for additional advance in brain tumor treatment.

Although traditional and advanced learning techniques support brain tumor detection they bring different methods to increase diagnostic precision and effectiveness [2]. Image enhancement through denoising and contrast change plus feature selection using histogram methods and wavelet tools make up standard methods. The system uses Support Vector Machines (SVM), Random Forests, K-Nearest Neighbors (KNN), and Logistic Regression algorithms for tumor classification from the obtained features. After segmentation the computer applies morphological transformations to enhance the segmentation results. Advanced methods of deep learning have become essential for detecting tumors today. CNNs use image data to develop their own basic features without the need for manual assistance. Encoder-decoder architectures and GAN models boost tumor boundary detection and make more diverse training samples helping the developed medical systems perform better. Models that were initially trained on different tasks can be modified with transfer learning to spot brain tumors when there are not enough marked datasets. Researchers currently blend machine learning and deep learning approaches to make best use of both strategies [3]. Despite strong processing capacity the system needs more accurate data sources while also updating its output for users to understand better. Different technologies improve brain tumor detection today yet main advancements come from mixing traditional and advanced algorithms.

Problem Statement

Segmentation of brain tumor is in demand in medical image analysis because identification and segmentation of tumor locations is essential for establishing an effective equipments of diagnosis, treatment and monitoring. Unfortunately, the problem is dexterous in that anatomies of brain tumours vary from one patient to another exhibiting different shapes, sizes and even appearances. Reliable segmentation of the tumors is typically a challenge of traditional approaches due to tumors of irregular shape or positioning close to crucial parts of the brain. Besides that, the conventional deep learning architecture fails to maintain a high segmentation accuracy while the spatial information is lost with the down sampling in encoder decoder models. However, with the development of more advanced architectures e.g., ResNet network they have been able to tackle these issues to some levels, and it has become necessary to combine these models with an insightful loss function like Dice Loss in order to deliver the exactness and precision of tumor segmentation [4]. To address such problems of challenges,

Volume 38 No. 2s, 2025

ISSN: 1311-1728 (printed version); ISSN: 1314-8060 (on-line version)

the study will propose a skip connected ResNet-18 encoder-decoder network [5] with Dice Loss to enhance the accuracy and efficiency of the process of brain tumor segmentation.

Motivation

It is motivated by a lack of current methods that can effectively deal with complex tumor structures in the brain tumor segmentation problem. Although the traditional approaches are successful, they usually fail to reach the level of high accuracy in segmentation, because of noise, irregularities and tumor shape variability. However, due to the downsampling in the encoder part, most encoder-decoder networks tend to lose spatial details while generating segmentations. To solve this problem, the ResNet-18 architecture, based on residual connections was suggested that prevents the problem of vanishing gradient, letting the networks go as deep as possible. The model can preserve important spatial information by applying skip connections between the encoder and the decoder, which helps to improve the segmentation accuracy. Furthermore, the usage of Dice Loss also aids in improving the segmentation performance which directly optimizes for the overlap of predicted with ground truth tumor regions. In this research we aspire to devise a new model which will improve the brain tumor segmentation's reliability and accuracy that will later assist with early diagnosis and also in improving treatment for the patients.

The rest of the paper as follows. A brief background about tumor segmentation on MRI images is given in section 2. Bottomline of methodology used in the study is shown in section 3. In Section 4, we provide dataset and performance evaluation metrics applied used, and comparison against baseline methods' results. The section 5 has conclusions regarding the work.

2. Background Study

Other works of the same issue and those devoted to other types of brain tumors are valuable due to working as the source of basic tricks and methodologies that made the current more accurate and quick models possible. Segmenting brain tumors is difficult based on previous research since tumors are of all shapes, sizes and positions and worrisome to preserve spatial details in encoder decoder networks due to the downsampling process. Although studies, particularly incarnations of deep learning, including convolutional neural networks (CNNs) and encoder-decoder architectures, have addressed these concerns, such approaches have struggled in the area of complex tumor shapes or small tumor area relative to the background. In addition, the loss function such as Dice Loss is used to augment segmentation that maximizes overlap in the predicted and ground truth tumor regions. With skip connections, ResNet architectures prove to be capable of achieving great enhancements to preserve feature information in passing through the network. This work uses the study of these other works to extrapolate these advanced techniques (a skip connected ResNet-18 encoder decoder network combining it with Dice Loss) to increase the precision of segmentation which is vital towards improving

Volume 38 No. 2s, 2025

ISSN: 1311-1728 (printed version); ISSN: 1314-8060 (on-line version)

diagnostic precision, guidance for treatment decision-making and subsequently patient survival..

Shravan, Venkatraman [6] suggests a new deep learning method to help with detecting, and segmenting gliomas from brain MRI images. The authors recommend a synergy between SeNet (Squeeze-and-Excitation Networks) and ResNet (Residual Networks) into an encoder decoder structure. In particular, the SeResNet 152 is employed as the backbone of their model. The functions of this integration include the improvement of the feature extraction feature and the accuracy of segmentation by using Channel Attention Mechanism and Deep Feature Extraction. SeNet introduces a Channel Attention mechanism to allow the network to pay attention to the most informative features in an attempt to recalibrate the channel-wise feature responses. Residual connections in ResNet allow for it to be trained with deeper networks and item.Business learn more complicated patterns in the data. The model picks up these hierarchical features in hierarchical manners and combines these architectures, through an encoder decoder framework. Some performance metrics were adopted and the following benchmarks to estimate the proposed model which includes Dice Coefficient: 87 % Accuracy: 89.12 % Intersection over Union (IoU) 88 % and mean IoU 82 % The value of these metrics evidences a good share of conforming to correctly segregate glioma regions from MRI scans. A combined encoder-decoder model with SeResNet being the basic model is proposed and demonstrated with high efficacy in segmenting glioma. The basis will be Deep learning residual and channel attention. Nevertheless, the paper fails to assess the model across a broader spectrum of clinical situation and variation of tumor. In addition, unlike most state-of-the-art methods there is no comparisons with other methods and the lack of a discussion on the computational efficiency of the proposed method may make it difficult for the proposal to be applied in practical settings.

The goal of Zhang, Wenbo, et al.[7] research is to enhance the segmentation accuracy of 3D MRI brain tumors using an innovative architecture of deep learning. The dominant and most prevalent form of brain tumors is gliomas. In order to have a successful diagnosis and treatment planning, it is necessary to have accurate segmentation of these tumors in the MRI images. However, manual segmentation is a highly tedious process and is full of inconsistencies. Deep learning has indeed made it possible to do segmentation automatically but most of the existing methods work only at the level of 2D, thus leading to the issue of suboptimisation if the brain tumor happens to be 3D. Such challenges as voxel imbalance and variations in tumor size and location make it further complicated to have accurate segmentation. To address these issues, we apply ME-Net that is a multi-encoder, and single decoder. The network has four distinct encoders (multi-encoder design) for each of the four MRI modalities (T1, T1c, T2, and FLAIR). There is also permission for modal specific feature extraction in this design, thus providing the network with more opportunities to detect number of different tumor characteristics. The output of the four encoders is then combined, processed by the common decoder synthesizing the amalgamated features in order to output the final segmentation. A novel loss function, Categorical Dice, is brought into the fold. It makes different regions of the

Volume 38 No. 2s, 2025

ISSN: 1311-1728 (printed version); ISSN: 1314-8060 (on-line version)

tumor receive different weights in this case to address the issue of voxels imbalance thus enhancing the performance of segmentation across the various sub regions of the tumor.

The performance of MENet was measured using the BraTS 2020 Challenge dataset that is a well-known brain tumor segmentation benchmark. Specifically, the following Dice scores were obtained using the model: WT (0.70249), TC (0.88267), ET (0.73864). Moreover these results demonstrate that ME-Net competes with state-of-the-art techniques and specifically it compares well on the tumor core segmentations. In this work, ME-Net delivers a strong measure for 3D brain development segregation utilizing modality specific encoders with an appropriately structured loss capacity to address certain primary complexities related to medical picture analysis. It is well suited for clinical use to diagnose and plan for its treatments from its architecture and performance.

Saqib Qamar, Parvez Ahmad, and Linlin Shen[8] considers problem of segmentation of brain tumor from 3D MRI scan with aim of improve the segmentation accuracy using advanced deep learning model. A new improved 3D UNet architecture, HI-Net (Hyperdense Inception 3D UNet), which includes the Factorized 3D Convolutions, where a standard 3D convolution is split into several branches to process extracted features from the orthogonal planes (axial, sagital and coronal) separately. Inception modules with residual connections are used in the Residual Inception Blocks in order to facilitate the extraction of multi-scale features. Hyperdense Connections further strengthen dense reuse of features and hence connections between and inside layers whenever they occur, making the gradient able to pass through the nn more easily. It is based on evaluating it with the BraTS 2020 dataset, a multimodal MRI that is annotated with Whole Tumor (WT), Tumor Core (TC), Enhancing Tumor (ET). The Performance Metric as Dice Similarity Coefficient (DSC) scores on WT (0.87494), Tumor Core (0.83712) and Enhancing Tumor (0.79457). High sensitivity and specificity in all the tumor regions demonstrated the reliability of the segmentations.

To relieve a radiologist's burden, in 2015, Huang, Wang, Zhang, Li, and Dong [9] proposed automated brain tumor segmentation in MRI images with the purpose of high accuracy. The Proposed Methodology had incorporated a parallel multi-scale feature-fusing architecture with feature extraction network (FEN) that extracts the features of a tumor at different levels. Multi scale Feature Fusing Network (MSFFN), Alternatively, it joins the feature in parallel from various scales to create rich feature. I developed two hybrid loss functions that assist in leveraging class imbalancing issue as HL1 and HL2. HL1 is the amalgamation of cross entropy loss and recall loses for complete, core and enhancing tumor regions. HL2 is achieved by overlapping Dice loss with recall losses that apply to the same regions. We tested the method against the BRATS 2015 dataset, which has 274 cases for training (54 low-grade, 220 high-grade tumors) and 110 test cases whose ground truth was not disclosed. There are four MRI sequences for each case, namely T1, T1-contrast, T2, and FLAIR. Metrics related to evaluation were the Dice Similarity Coefficient (DSC), Positive Predictive Value (PPV), and Sensitivity. DSC has been to achieve 0.86 for complete tumor region and 0.73 for tumor core region, 0.61 for enhancing tumor region, model size is compact i.e, 6.3 MB. It performed better than other methods which are state-of-the-art but which have

Volume 38 No. 2s, 2025

ISSN: 1311-1728 (printed version); ISSN: 1314-8060 (on-line version)

no post processing for the complete segmentation of tumors. The fusion of multi-level features due to parallel structure ensures better accuracy of segmentation. To mitigate the class imbalance, the hybrid loss functions are used to enhance the sensitivity in the detection of tumor regions. It is demonstrated that the method can be potentially used on other cases of medical image segmentation.

A suitable and automated segmentation of the brain tumor was the approach in which Wang G., Li W., Aertsen e.t. [10] developed based on the cascaded deep learning with anisotropic convolutions approach. Provided a cascade of three neural networks for segmenting three different tumor subregions namely Whole Tumor (WT), Tumor Core (TC), and Enhancing Tumor Core (ET) that contain only enhancing suprathreshold voxels. Detailed 3D context is obtained with ACNNs while computing cost is pushed down. Takes advantage of in plane and cross plane characteristics through the application of 2D/3D convolutions (hybrid). A multi view fusion approach is used to integrate predictions of axial, sagittal and coronal views and provide robustness. The test time augmentation technique is employed when the inference time has to increase accuracy by applying transforms at inference time. It has been tested on the BraTS 2017 dataset that contains multimodal MRI scans and the references label. On the performance evaluation, it had competitive Dice scores across all tumor sub regions. It was better than many baseline and state of the art methods, as it was ranked in BraTS 2017 challenge rankings. The scheme of effective anisotropic convolution enables efficient use of memory, as well as effective use of a cascade strategy to accomplish the processing of a complex tumor structure in stages. The cascaded anisotropic CNN approach obtains and maintains adequately good performance and computational expenses suitable for verities in the real-world clinical endeavors.

Juhong Tie, Hui Peng, Jiliu Zhou [11] introduced a method based on the combination of DenseNet and ResNet into a 3D U-Net structure to enhance accuracy in brain tumor segmentation of MRI images. A new 3D U-Net architecture is constructed based on Dense Encoder Blocks and Residual Decoder Blocks. To increase feature propagation, alleviate vanishing gradients and cap the receptive field, it uses Dense Encoder Blocks, which utilize dense connections. Segments consist of residual Decoder Blocks, having residual connections to ensure more flow of gradients and improved segmentation results. Each layer of Dense Encoder Blocks takes inputs from all the preceding layers promoting reuse of feature and good flow of gradients and the ability of the net work to catch complex features the few parameters. The remarkable changes of Residual Decoder Blocks include the mainstay skip connections, which add nothing more than plain addition of input of a layer to its output, the aim is to assist in learning of identity mappings and convergence. A key evaluation aspect of the model is done using the (multimodal) MRI scans with marked tumor parts of the BraTS dataset that came out in 2019. Whole tumor (WT): Dice Similarity Coefficients. TC (Tumor Core): 0.901, ET (Enhancing Tumor): 0.815, SUVmax (Tumor ROI): 0.766. In the demonstration, the proposed model beats the traditional 3D U-Net when it comes to segmenting different sub regions of tumors. It demonstrated the increased accuracy and robustness for managing complex structure of tumor. High-dimensional and residual connections layered using a 3D U-Net architecture

Volume 38 No. 2s, 2025

ISSN: 1311-1728 (printed version); ISSN: 1314-8060 (on-line version)

contribute to improving feature learning and segmentation performance. It also claims to be applicable to the clinical setting in automated diagnosis of brain tumor and planning of treatment.

Aboussaleh I, Riffi J [12] and colleagues suggested an improved U-Net based model for segmentation of MRI images (brain tumor) through incorporating innumerable encoders and attention mechanisms. The architecture uses three pre-trained CNNs - VGG-19, ResNet50, and MobileNetV2 - as encoders to yield rich and variable features. A Bi-Directional Feature Pyramid Network (Bi-FPN), on the other hand, merges multi-view features of every encoder for boosting spatial and contextual knowledge. The decoder has focus modules that help in segmentation accuracy by focusing on the relevant features to suppress noise. This configuration of multi-encoders takes advantage of superrelative properties of other different CNN to better represent intricate tumor structures. On the basis of the BraTS 2020 dataset, the model has outperformed the traditional variants of the U-Net in terms of Dice Similarity Coefficient, IoU, and precision/recall for the subregions of tumors. It precisely segmented the entire tumor, tumor core, and enhancing regions. The architecture performed significantly better accuracy and computational efficiency relative to current state-of-the-art approaches. Its benefits make it very suitable for use in clinical settings where an accurate and reliable delineation of the tumor is needed.

Zhang, J.; Shen, X.; Zhuo, et al. [13] suggested an improved method of brain tumor segmentation in MRI by improving Fully Convolutional Neural Networks (FCNNs) and implementing Hierarchical Dice Loss function. Acknowledging the issues related to class imbalance and the complexity in tumour' nature (in particular gliomas), they have modified traditional FCNN prototypes by introducing inter-layer connections, expanding decoders, introducing residual structures, as well as introducing batch normalization to enhance the performance. Their novel loss function converts multi-class classification into binary classifications depending on the hierarchical tumor subregion relationships, which actually accounts for class imbalance. Trained on the BraTS dataset, the model exceeded the performance of traditional FCNNs with regard to precision, recall, mean IoU, and Dice Similarity Coefficient. It offered better accuracy in segmentation of whole tumors, tumor core, and enhancing areas. Architectural refinements and loss function came together for the artifacts of addressing tumor complexity and boundary delineation. Such an approach showcased high promise for clinical application situations where there was a need for precise and time-effective tumor segmentation.

Lijuan Yang et al. [14] suggested MUNet that leads to the combination of the strengths of local feature extraction of UNet and the modelling of brain global context abilities by Mamba in order to achieve better brain tumor segmentations. Traditional CNNs are good at capturing local details but bad for global context, transformers are good with global modeling but come with computational cost. The MUNet introduces the SD-SSM block where selective scanning and state-space modeling are combined in order to provide global as well as local learning from the features. The SD-Conv module brings the two options, i.e., SCCONV and depthwise separable convolutions, which improve efficiency by removing redundancies without adding

Volume 38 No. 2s, 2025

ISSN: 1311-1728 (printed version); ISSN: 1314-8060 (on-line version)

parameters. Skip connections help to implement multi-scale feature fusion and retain spatial details. A composite loss function—mIoU, Dice, and Boundary loss—seeks to optimize the segmentation quality as well as the boundary accuracy. Evaluation on BraTS2020, BraTS2018, and another isolated LGG dataset reported good Dice and competitive Hausdorff95 performances. In terms of efficiency, MUNet performed with superior speed compared to SwinUNet and TransUNet, having only 7.27M parameters and 140.97 GFLOPs. All the same, there are challenges that arise in interpretability, fear of overfitting, and also segmenting very heterogeneous tumors. Future improvements are recommended to incorporate improvements in boundary detection and the use of data augmentation and transfer learning.

Akshya Kumar Sahoo, Priyadarsan Parida, et al. [15] developed an intelligent system for automatic brain tumor detection for 2D contrast-enhanced MRI images utilizing two-stages: segmentation followed by classification. Segmentation was done using a U-Net with the backbone of a residual network whereas classification of glioma, meningioma, and pituitary tumors was carried out using a YOLOv2 transfer learning approach. The model reported a high Segmentation accuracy (99.60%), and Classification accuracy (97%) and higher than the state-of-the-art techniques. Some of the main areas of contribution include the fusion of segmentation and classification into a single pipeline and the effective deployment of transfer learning for medical imaging. The results of the system were good in terms of sensitivity, specificity, precision, and Dice score. It has important feasibility for clinical use in diagnosis and treatment decision in part. Future work proposes further development of the idea to the 3D image to increase accuracy and vice versa, as well as considering other deep learning models. It is recommended that further validation is done on larger and more varied datasets to allow for generalizability.

Sedigheh Sina et al. [16] suggested a method of automated segmentation of Glioblastoma Multiforme (GBM) in MRI images using the DeepLabv3+ structure with pre-initialized ResNet18 weights. The model was trained on 293 HGG cases using the BraTS 2020 dataset, which had multimodal MRI scans (T1ce and FLAIR). Manual annotations by expert neuroradiologists were employed as ground truth to demarcate the tumor subregions during the process, which included: enhanced tumor, edema, necrotic regions, and normal regions. The network was optimized by various hyperparameter experiments and performed best in epoch 37 with 97.53% Global accuracy at a loss of 0.14 and higher than 90% sensitivity to find out enhanced tumors. The Deep-Net model scored high on segmentation accuracy, especially for the tricky GBM one. The study illuminates the fact that integrative DeepLabv3+ and pre-trained ResNet18 is a strong and viable option for utilizing semantic segmentation in medical imaging.

In their review, M.K.H. Khan and colleagues [17] discussed the application of machine learning (ML) and deep learning (DL) methods in tumor segmentation from MRI data, comparing the advantages and challenges and the emerging trends of the subject under discussion. Common algorithms that are mentioned in comparison with ML are thresholding and edge detection, as well as GMM, SVM, and FCM, which deliver a good range of accuracy while also failing to perform well with noise and variability. DL methods, especially CNNs and U-Net, demonstrate outstanding successes in diagnosing and serendipitous tumors but have

Volume 38 No. 28, 2025

ISSN: 1311-1728 (printed version); ISSN: 1314-8060 (on-line version)

high needs in big annotated data sets and computing power. The analysis of the segmentation methods was based on datasets such as BraTS (2012–2021), TCIA, BrainWeb, and IBSR. Despite other models, U-Net always does a better job in depicting detailed structures of tumors. It is increasingly preferred to use ML and DL methods in combination to take advantage of the two's strengths. Some of the key limitations include generalization of the model to different patterns of tumors, the lack of interpretability, and the implementation of powerful hardware. The future efforts are to develop diverse, annotated datasets, enhance the real-time performance and develop user-friendly systems for clinical integration thus make them acceptable in hospital settings.

From the above study, it is identified that, several limitations in brain tumor segmentation using deep learning have been found consistently. Currently, approaches are lacking in generalizability across different tumor type, clinical conditions and datasets and limited in the analysis of robustness towards artifacts and variations in the model. However, there has often been a strong emphasis on segmentation accuracy to the extent that much less attention is paid to other essential factors like computational cost, efficiency, and deployment feasibility on a real-world system. Due to high architectural complexity and high required computational resources, many models cannot be used in real-time in a clinical application. Further on, several methods exhibit a risk of overfitting, are often not scalable and/or not interpretable – which are both critical for clinical trust. Additionally, some of the studies do not utilize all possible MRI modalities or are restricted to 2D images Cyprus reducing their scope for analyzing the tumor in 3D. Additionally, proposed innovations are hard to validate as there are no comparisons with state-of-the art techniques, and there are not enough ablation studies. Thus, there are still challenges with regard to data availability, efficiency, interpretability, and generalization in the field overall.

3. Proposed Work

3.1 ResNet-18

ResNet-18, on the other hand, is a deep convolutional neural network that replaces some of these problems with residual learning to alleviate the challenges associated with training very deep networks [18]. ResNet-18 architecture is given as Figure.1 [19]. It has 18 layers consisting mainly of convolutional and identity shortcut connections that are responsible for the reduction in the vanishing gradient problem. The architecture is to be considered as starting by applying 7 × 7 conv then moving on to max-pool, which leads to a decrease in spatial resolution. This is then followed by four (Layer 1 to Layer 4) all have Layer 2 having 2 residual blocks with either two filter depths, 64, 128, 256, and 512. In another stage (other than Layer1), an initial down-sampling of the feature maps is done with stride2, and the rest of the blocks have dilations towards the respective dilation index. The second is a residual block, which includes two layers; the first being 3x3 convolution, batch normalization, and ReLU; the second is also 3x3 convolution, batch normalization, and ReLU. In every block, we apply skip connections which skip over onto the convolutional layers and hook back onto the output in order to promote gradient flow. Finally, a global average pooling is applied to it, so as to reduce the

Volume 38 No. 2s, 2025

ISSN: 1311-1728 (printed version); ISSN: 1314-8060 (on-line version)

dimensionality of the feature maps on this channel down to a single vector. Finally, among these, a fully connected layer provides the classification scores. Despite having a relatively low cost in terms of computation, ResNet-18 is able to achieve a strong performance that can be used for both academic and pragmatic ends.

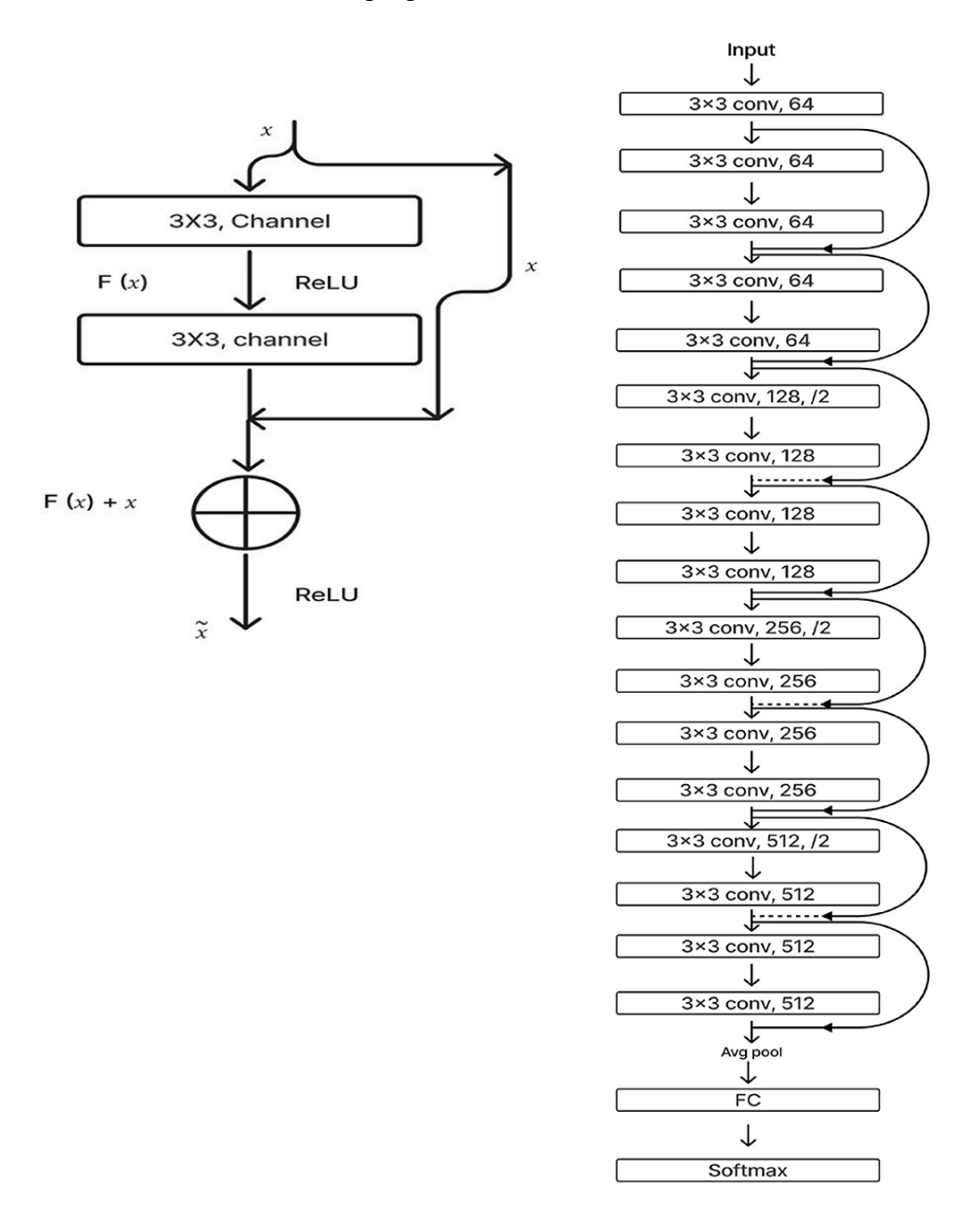


Figure 1. ResNet-18 architecture.

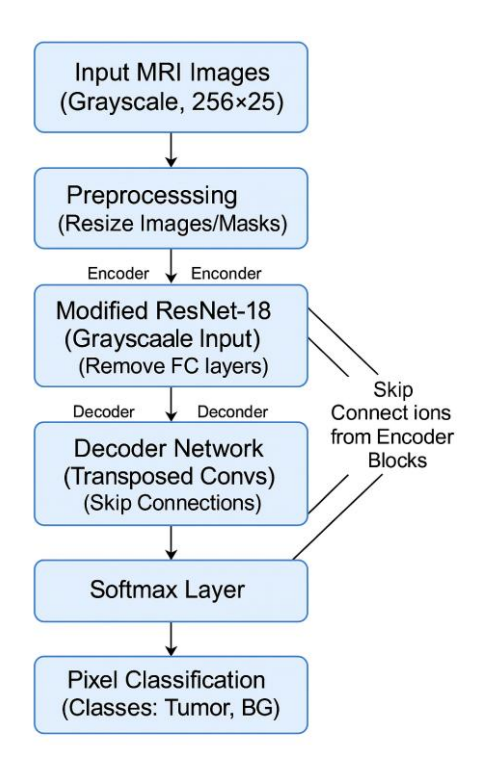
3.2 Proposed Methodology

The proposed methodology is based on developing a skip connected ResNet-18 Encoder Decoder network, optimized with Dice Loss in order to improve the accuracy and precision of tumor delineation with medical images. The first step involves the acquisition and preprocessing of brain tumor MRI images stabilizing typical problems of MRI like noise,

Volume 38 No. 2s, 2025

ISSN: 1311-1728 (printed version); ISSN: 1314-8060 (on-line version)

intensity variation, and other artifacts by typical standard processes of image normalization and denoising.



Segmented Tumor Mask

Figure 2. Block diagram of proposed method.

The novelty of the proposed method can be observed in the use of ResNet-18, a wide-spread known deep convolutional neural network deployed based on residual connections. The residual connections make the model learning deeper, more complex representations, and allows the model avoid the issue of vanishing gradients. The encoder – decoder architecture in this case performs feature extraction in which the encoder reduces the dimensions of the feature maps and retains the high level features and the decoder reconstructs the image by up sampling the feature maps to fill up all the empty spaces. An encoder and a decoder are linked via a skip connection to disseminate high-resolution spatial information to earlier layers of the network to later layers ensuring the maintenance of any important information as regards to the shape and the borders of the tumor in the process of down sampling.

A Dice Loss is added as an optimization goal and further enhances the accuracy of the segmentation [20]. As another form of metric, Dice Loss is the one which is far more specific in that it tries to transition into maximizing the overlap between the prediction made by the regarded model for the segmentation of the tumor with the ground truth. This variation of metric is more preferable, particularly to function as a way of assessing a model designed with the scope of predicting the tumor specifically out of the extensive border of the healthy tissue.

Volume 38 No. 2s, 2025

ISSN: 1311-1728 (printed version); ISSN: 1314-8060 (on-line version)

In this method, the ideas of residual learning, skip connections, and a loss function have been merged to impart it with the strength to be a good methodology toward brain tumor segmentation. The ultimate aim is to create more accurate segmentations to help better diagnose and treat patients leading to better patient outcome. Implementation approach of proposed method is shown in the block diagram Figure 2.

3.2.1 Pre-Processing

Image resizing appears to be the first step of the preprocessing phase in order to get images of the same resolution i.e (256 × 256) or (224 × 224) pixels depending on the input requirement of the network. This is important in ensuring that you will have consistent feature extraction, and an efficient batch processing. Once the resize is done in this step, a masking operation is conducted in which resize ground truth segmentation masks according to the segmentations of tumor regions are resized in the same manner as the input images are aligned pixel to pixel. This means masking aids in telling the model what is tumor vs non tumor and telling the model the spatial patterns. In training, the ResNet-18 embedder encodes deep level, and skip connection is used to save the fine level localization information. These features are gradually up-samples by the decoder to reconstruct a detailed segmentation map. The Dice Loss function works really well for imbalanced classes such as tumor and background as it calculates the overlap between the predicted mask and the ground truth, and prompts the model to properly segment both small and also irregular tumor regions. When using image resizing, you have uniformed inputs, and when using masks indicate the model exactly where to aim at during training.

3.2.2 Encoder Function

The encoder is an adapted ResNet-18, modified to be able to entertain 1-channel grayscale MRI inputs in place of standard RGB images. The parts for both convolutional feature extraction remain while the final fully connected (FC) classification layers are stripped away. We skip-linked encoder-decoder stages at matched stages: res4b_relu, res3b_relu, and res2b_relu are passed to the respective decoder layers. Therefore, this design enables us to retain high-level semantic as well as fine-grained spatial detail when up sampling which is very important for accurate segmentation of complex boundaries of brain tumour when segmenting them.

The encoder maps an input image x to a set of increasingly abstract feature maps. Each block inside ResNet-18 has a residual connection. Mathematically, each block can be represented as:

$$y = F(x, \{W_i\}) + x$$
 (1)

Where:

- x=input to the block (feature map),
- $F(x, \{W_i\})$ = residual function (typically two or three convolutions with batch normalization and ReLU),

Volume 38 No. 2s, 2025

ISSN: 1311-1728 (printed version); ISSN: 1314-8060 (on-line version)

- $\{W_i\}$ =weights of convolution layers,
- y=output of the block.

Structure of ResNet-18

The structure of ResNet-18 [21] which is shown in Figure.3, is composed of two main components: ResNet-18 contains two separate parts: its initial layers with subsequent stacks of residual blocks arranged in four stages. The first stages in the network receive raw images and generate fundamental image properties from them. It uses a 7×7 convolutional layer with a stride of 2 to detect basic image features including shape and texture. The network applies batch normalization to stabilize learning when it follows these steps. The ReLU activation function creates non-linearity for the network so it can understand intricate patterns. This next layer transforms the spatial inputs twice to achieve better results with minimal increase in computation demands.

After its starting layers ResNet-18 uses four stage blocks with two blocks each to reach eight blocks total [21]. Each residual block uses two 3×3 convolutional layers. Batch normalization and ReLU activate the results of each convolution except for the last 3×3 convoluted layer before it passes to the next block. Residual blocks are designed with a special connection that lets their input travel directly to their output. This identity mapping helps gradients navigate better through deep structures and fixes the problem deep networks usually have with vanishing gradients.

The four processing stages in this architecture regularly downscale spatial dimensions while adding more feature channels. The image resolution decreases across stages with corresponding filter increases from 56×56 with 64 features to 7×7 at 512 features. Each stage down sampled through two-layer block combinations where the first block implements a stride of 2 convolution and includes a 1×1 convolution in its shortcut path for dimension adjustment. The performance-relevant design choices in ResNet-18 led to its straightforward transition into deep models hence becoming a popular deep learning framework.

Residual Block Definition

Each residual block performs the following computation:

$$F(x) = W_2 \sigma(W_1 x) \tag{2}$$

Where:

- W₁, W₂ are convolutional filters,
- σ is ReLU activation.

With the skip connection, the final output becomes:

$$y = F(x) + x \tag{3}$$

The architecture enables networks to discover the residual mapping while reducing training time and enabling deep network training without performance loss.

Volume 38 No. 28, 2025

ISSN: 1311-1728 (printed version); ISSN: 1314-8060 (on-line version)

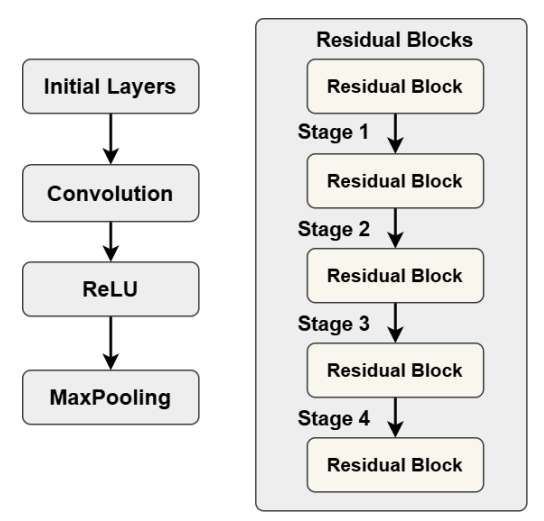


Figure 3. The structure of ResNet-18

3.2.3 Decoder and Skip Connections

In segmentation networks skip connections help keep spatial details intact after down sampling in the encoder phase.

- Feature maps are saved at each phase of the encoder process.
- The decoder combines saved maps with its own up sampled output during processing.

The formal definition of Skip Connection at Level *l* is

$$S_{l} = y_{l} \tag{4}$$

Where:

- S_l =saved feature map at level l.
- y_l = output of the encoder at level l.

Decoder Structure

The decoder rebuilds full-resolution segmentation maps by using transposed convolution networks called deconvolutions to expand the feature maps. Through this design the architecture builds output quality step by step. The decoder connects to encoder output data (via skip connections) to both keep detailed spatial information and enhance its ability to segment images.

3.2.4 Loss Function: Dice Loss

The model is trained using the Dice Loss [20], which is particularly useful for medical imaging segmentation tasks, where class imbalance (e.g., small tumor vs. large background) is a concern. The Dice Loss helps address class imbalance and matches predicted regions more accurately with their ground truth in medical image segmentation. The standard Dice Loss formula represented as:

Volume 38 No. 2s, 2025

ISSN: 1311-1728 (printed version); ISSN: 1314-8060 (on-line version)

Dice Loss=1-
$$\frac{2|P \cap G|}{|P|+|G|}$$
 (5)

Where:

- P=predicted segmentation
- G = ground truth segmentation
- $|P \cap G|$ = intersection (common area) between prediction and ground truth

It effectively penalizes both misclassification of positive samples as negative and vice versa, which is beneficial in applications such as tumour segmentation.

Pixel-Wise Sum Formulation dice loss is represented as:

Dice Loss=1-
$$\frac{2\sum_{i}p_{i}g_{i}}{\sum_{i}p_{i}^{2}+\sum_{i}g_{i}^{2}}$$
 (6)

Where:

- p_i =predicted probability at pixel i.
- g_i =ground-truth label (0 or 1) at pixel i.

This formulation is convenient for implementing in code with tensor operations and is greatly efficient for measuring the overlaps in segmentation tasks.

Decoder Fusion Step (Transposed Convolutions + Skip Fusion)

The saved feature maps from the encoder (via skip connections), are fused with upsampled decoder features for the sake of spatial context during decoding. The decoder fusion equation is represented as

$$d_{l} = Decoder(d_{l+1}) + s_{l} \tag{7}$$

Where:

- d_1 = decoder feature at level l.
- s_l = corresponding skip connection (encoder feature at level l)

The fusion allows the decoder can retrieve high-resolution details from encoder layers of the network for enhanced segmentation accuracy.

3.2.5 SoftMax Layer

The SoftMax layer helps the network transform its raw logits into probabilities that show the distribution between background and tumor classes [22]. With this step the model demonstrates how confident it is about placing each pixel into its correct category. SoftMax adjustments help relate predicted outputs across pixels so users can set thresholds for better decision-making during segmentation. Models need SoftMax outputs during training to compute loss functions such as cross-entropy and Dice Loss which require probability

Volume 38 No. 28, 2025

ISSN: 1311-1728 (printed version); ISSN: 1314-8060 (on-line version)

estimation. Basic SoftMax processing makes it possible for the network to learn properly and produce reliable tumor segmentation results.

For an input vector of logits $z = [z_1, z_2, ..., z_K]$ corresponding to K classes, the **SoftMax** function outputs a probability distribution:

$$\sigma(z) = [\sigma(z_1), \sigma(z_2), \dots, \sigma(z_K)]$$
(8)

Where: $\sigma(z_i) = \frac{e^{zi}}{\sum_{j=1}^{K} e^{z^j}}$ for each i = 1, 2, ..., K

This guarantee that the output values sum to 1 and also represent valid probabilities for classification tasks.

Here, e^{zi} raise each logit value to the power of the element value, indicating higher values. The denominator $\sum_{j=1}^{K} e^{zj}$ makes certain that the predicted probabilities in every class add up to 1. Thus, each of them is in the interval (0, 1), where each number corresponds to the probability of class i.

In the case of Brain Tumor segmentation with 2 classes, namely background and tumor, the SoftMax provides two probabilities for each pixel of a given image to allow the network distinguish between which class the pixel is most likely belongs to.

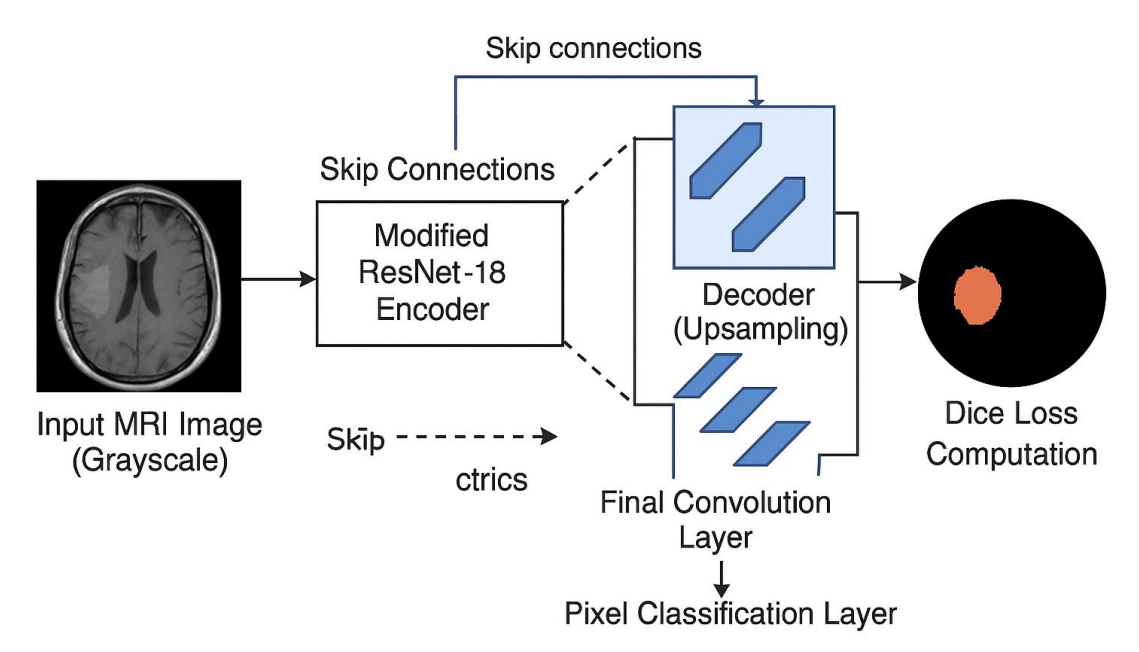


Figure 3. Enhanced Brain Tumor Segmentation framework using a skip-connected ResNet-18 Encoder-Decoder Network with Dice Loss.

When it comes to deep learning, hyperparameters will be very vital, as they will have a significant impact on the performance of your model and also its generalization. Tuning properly enables the optimization of not only the learning rate and the batch size (see Batch

Volume 38 No. 2s, 2025

ISSN: 1311-1728 (printed version); ISSN: 1314-8060 (on-line version)

Size), but also the network structure for it not to be underfitting, overfitting [23]. This ensures that data input is parsed in a suitable way for the model so that the learning of the models occurs and the model convergences faster. Even with advanced models, they can be destroyed while tuning. Table 1. presenting hyper parameters declared for train the model.

Table 1. Hyperparameters and configurations used in the proposed model.

Hyperparameter	Value	Description		
Learning Rate	1e-4	Initial learning rate for the Adam optimizer		
Mini Batch Size	8	Number of training samples in each mini-batch		
Num Epochs	30	Number of times the model will see the full training dataset		
Image Size	[256 256]	Input size for MRI and mask images (images are resized)		
Normalization	'Zerocenter'	Input images are normalized using zero centering		
Optimizer	'Adam'	Optimizer used for training		
Shuffle	'Every-Epoch'	Shuffles data after each epoch		
Execution Environment	'Auto'	MATLAB chooses between CPU and GPU based on availability		
Transposed Conv Stride	2	Stride used in all transposed convolutional (upsampling) layers in the decoder		
Transposed Conv Filter Size	4×4	Filter size for all decoder layers (deconvolutions)		
Decoder Channels	[256, 128, 64, 32, 2]	Number of output channels used in each decoder layer		

4. Result and Analysis

4.1 Dataset Collection

For the research, authors used the Brain Tumor dataset from Southern Medical University in Guangzhou that they collected from [24] and [25]. As demonstrated in Figure.4, data are given by 233 patients who brought 3064 medical scans. All the pictures in the dataset lie within the threshold as belonging to any of the 3 tumor classes: According to Southern Medical University's brain tumor data, there are three different types of the tumors, namely meningioma, glioma and pituitary representing the tumor groups for 23.11%, 30.35% and 46.54% respectively to the overall cases. According to the dataset, there is a single slice that has 512 pixels. Figure 5 is a presentation of the transformed images and masks which in their original form were in .MAT format and currently in .PNG format.

Volume 38 No. 28, 2025

ISSN: 1311-1728 (printed version); ISSN: 1314-8060 (on-line version)

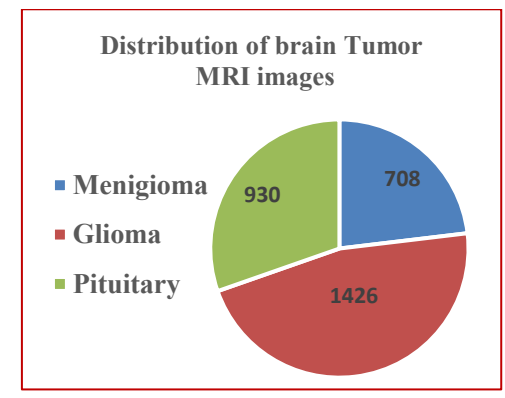


Figure 4. Composition of tumor images in dataset.

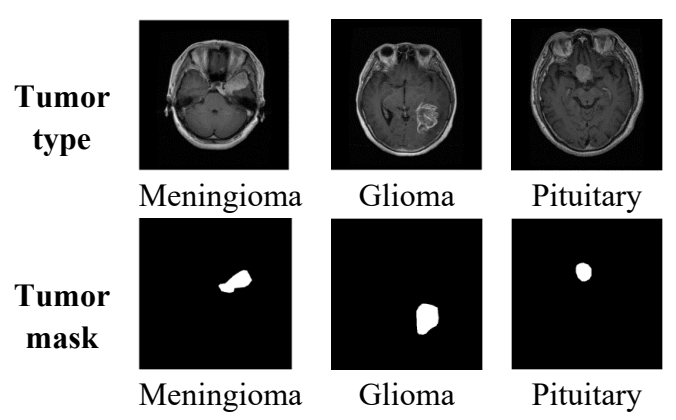


Figure 5. Brain MRI scans with tumor region masks.

4.2 Performance metrics

Dice Similarity Coefficient (DSC) also called Dice Score and Jaccard Index (JI) are important measures for the evaluation of the segmentation accuracy in medical imaging since they measure the overlapping of the predicted and the ground truth regions [26]. The DSC becomes very useful in a medical setting because of its sensitivity to small target regions. These high scores on these measures signify credible segmentation, which is paramount important for clinical decision-making. In addition to segmentation metrics, the confusion matrix is used for evaluating the performance of classification by representing a true/false positive and negative ratios to calculate accuracy, precision, recall, F1-score, and false positive rate (FPR) [27]. This matrix allows one to see how well a model classifies validation data. True positives and negative values represent correct predictions, while false positives and false negatives will represent incorrect predictions. Other performance indices are sensitivity, specificity, and area under ROC curve. These are obtained with standard equations to generally assess the AI model's performance effectiveness in diverse areas of performance. Equations numbered from 9 to 14 corresponds to performance metrics.

Dice Similarity Coefficient (DSC)=
$$\frac{2 \times |A \cap B|}{|A| + |B|}$$
 (9)

Volume 38 No. 28, 2025

ISSN: 1311-1728 (printed version); ISSN: 1314-8060 (on-line version)

Jaccard Index (JI) =
$$\frac{|A \cap B|}{|A \cup B|}$$
 (10)

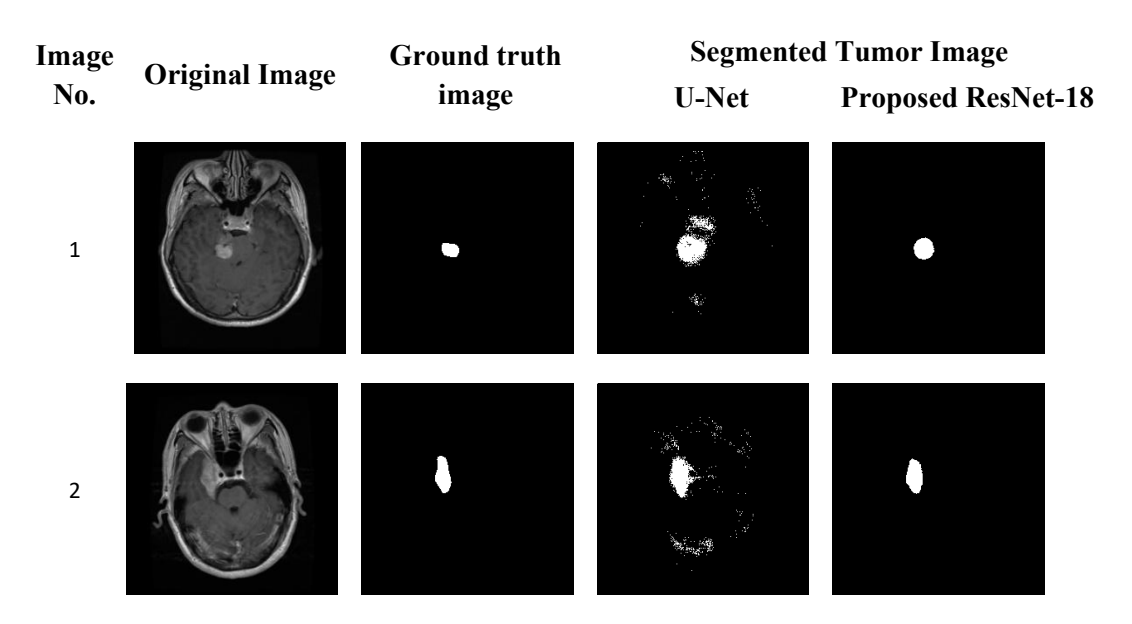
$$Precision = \frac{TP}{TP + FP} \tag{11}$$

$$Recall = \frac{TP}{TP + FN} \tag{12}$$

$$Accuracy = \frac{TP + TN}{TP + TN + FP + FN} \tag{13}$$

$$F1-Score=2 \times \frac{Precision \times Recall}{Precision + Recall}$$
 (14)

The evaluation of segmentation and classification performance parameters are shown in Table 2 and 3. Figures numbered from 7 to 12 showing the graphical analysis of segmentation and classification performance parameters. The proposed model demonstrates better results than the U-Net across measurement sets except for one occasion. Proposed model reaches 0.87% higher accuracy than the original U-Net design. The proposed system shows a 46.99% boost in accuracy which means it detects fewer false positive cases. Using both F1-score and Dice metrics we found a 28.27% enhancement in object detection accuracy and quality. The new model matches 44.98% more closely with expert-initialized marker positions when compared to ground truth information. Despite U-Net ranking better for recall by 0.84% our model surpassed every other performance metric leading to superior total segmentation results. The research shows that proposed model achieves better segmentation outcomes than other approaches because it limits errors and improves area matching specificity.



761

Volume 38 No. 2s, 2025

ISSN: 1311-1728 (printed version); ISSN: 1314-8060 (on-line version)

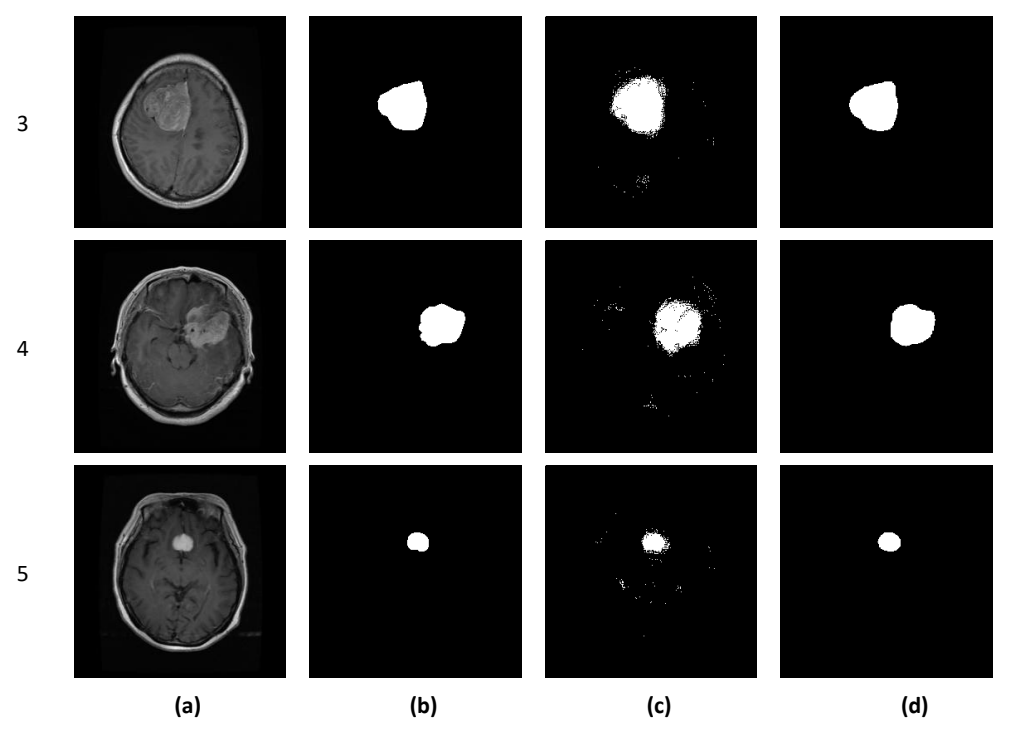


Figure 6. Segmentation results of U-Net and proposed model.

Table 2. DSC and JI parameter evaluation between U-Net and Proposed model.

Image	Γ	Dice Score	Jaccard Index		
	U-Net	Proposed Model	U-Net	Proposed Model	
1	0.3421	0.6966	0.2063	0.5345	
2	0.6084	0.9060	0.4372	0.8282	
3	0.8667	0.9801	0.7647	0.9609	
4	0.8618	0.9654	0.7572	0.9331	
5	0.8341	0.9587	0.7154	0.9207	

Table 3. Accuracy, Precision, Recall and F1-Score results between U-Net and Proposed model.

Image	Accuracy		Precision		Recall		F1-Score	
	U-Net	Proposed	U-	Proposed	U-	Proposed	U-	Proposed
		Model	Net	Model	Net	Model	Net	Model
1	0.9832	0.9963	0.2080	0.5536	0.9630	0.9394	0.3421	0.6966
2	0.9885	0.9982	0.4462	0.8910	0.9559	0.9216	0.6084	0.9060
3	0.9879	0.9984	0.7747	0.9721	0.9835	0.9881	0.8667	0.9801
4	0.9898	0.9977	0.7792	0.9768	0.9640	0.9543	0.8618	0.9654
5	0.9972	0.9994	0.7428	0.9444	0.9509	0.9734	0.8341	0.9587

Volume 38 No. 2s, 2025

ISSN: 1311-1728 (printed version); ISSN: 1314-8060 (on-line version)

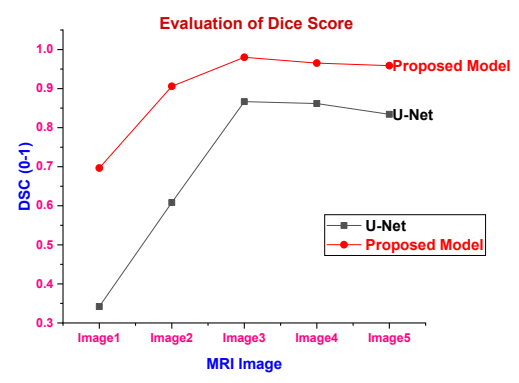


Figure 7. Dice Score analysis between U-Net and Proposed Model

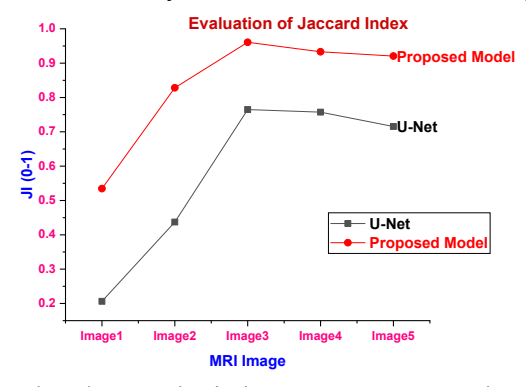


Figure 8. Jaccard Index analysis between U-Net and Proposed Model

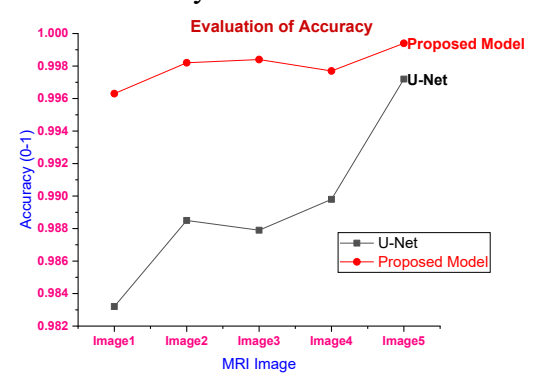


Figure 9. Accuracy analysis between U-Net and Proposed Model

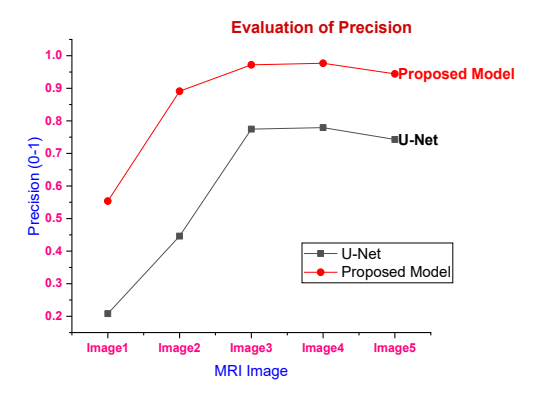


Figure 10. Precision analysis between U-Net and Proposed model

Volume 38 No. 28, 2025

ISSN: 1311-1728 (printed version); ISSN: 1314-8060 (on-line version)

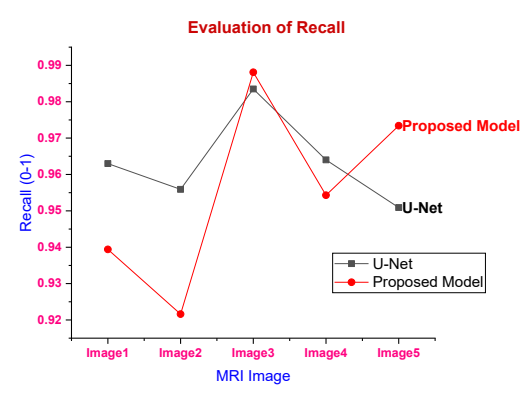


Figure 11. Recall analysis between U-Net and Proposed Model

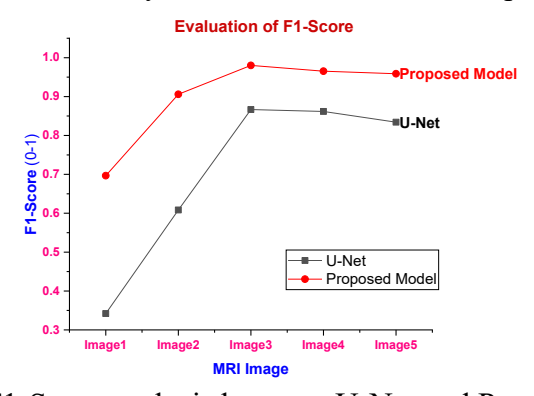


Figure 12. F1-Score analysis between U-Net and Proposed Model

The evaluation of segmentation and classification performance parameters are shown in Table 2 and 3. Figures numbered from 7 to 12 showing the graphical analysis of segmentation and classification performance parameters. The proposed model demonstrates better results than the U-Net across measurement sets except for one occasion. Proposed model reaches 0.87% higher accuracy than the original U-Net design. The proposed system shows a 46.99% boost in accuracy which means it detects fewer false positive cases. Using both F1-score and Dice metrics we found a 28.27% enhancement in object detection accuracy and quality. The new model matches 44.98% more closely with expert-initialized marker positions when compared to ground truth information. Despite U-Net ranking better for recall by 0.84% our model surpassed every other performance metric leading to superior total segmentation results. The research shows that proposed model achieves better segmentation outcomes than other approaches because it limits errors and improves area matching specificity.

4.3 Comparison with state-of-the-art methods

Table 4. Comparative analysis of classifier efficacy of various models.

Ref No.	Models	Accuracy	F1-score	Recall	Precision
Ilani, M. A., Shi, D. et al. (2025) [28]	3-Layer CNN	98	98	98	98
	EfficientNETB4	98.31	98	98	98
	VGG19	97.72	97	97	97
	InceptionV3	97.27	97	97	97

Volume 38 No. 2s, 2025

ISSN: 1311-1728 (printed version); ISSN: 1314-8060 (on-line version)

	U-Net	98.56	99	99	99
H. A. Shah et al (2022) [29]	EfficientNet-B0	98.8	98.9	99.5	99.4
Mostafa, A. M., Zakariah, M. et al. (2023) [30]	Deep CNN	99.21	-	96	99
Proposed Model	ResNet-18	99.8	95.25	95.9	94.61

Table 5. Comparative analysis of segmentation efficiency of various models

Ref No.	Model	Dice	Jaccard
		Score	Index
F. J. D. Pernas, M. Martínez-Zarzuela et al. (2021)	CNN-based	0.828	-
[31]			
B. V. Isunuri and J. Kakarla (2020) [32]	U-Net with AT	0.6239	-
S. Tripathi, A. Verma et al.(2020) [33]	SegNet	0.9332	0.8827
W. Huang and J. Wang et al. (2022) [34]	DFP-Unet	0.8169	-
A. K. Sahoo, P. Parida et al. (2023) [35]	Residual-Unet	0.9011	-
A. Ingle, M. M. Roja et al. (2022) [36]	Residual101-Unet	0.8369	0.85
B. Kumar, R. Panda et al. (2020) [37]	QuickTumorNet	0.724	-
C. Öksüz, O. Urhan et al. (2021) [38]	DeepLab with pre-	0.8091	-
	trained		
Z. Sobhaninia, S. Rezaei et al.(2020) [39]	Cascadeddual-	0.8003	-
	scale LinkNet		
A. Rehman, S. Naz, et al. (2019) [40]	SegNet VGG16	0.9314	0.7622
Saifullah, S., Dreżewski, R. et al. (2025) [41]	ResUNet50	0.9553	0.9151
Proposed Model	ResNet-18	0.9525	0.9107

Different deep learning models tested on Figshare dataset [24] achieve their classification results as shown in Table 4. Both Deep CNN model [30] and EfficientNet-B0 model [29] demonstrate excellent results with accuracy rates of 99.21% and 98.8%. While U-Net was built for segmentation tasks it achieved impressive classification results at 99% F1score and recall. The proposed method achieves 99.8% accuracy which proves its better ability to handle new datasets. Within the comparison set the model achieved lower efficiency in detection but invested in reducing false positive diagnoses which represents a very important function for medical applications. The proposed model achieves both outstanding accuracy and adequate error management making it an effective solution.

The evaluation of present segmentation approaches (Figshare dataset) uses Dice Score and Jaccard Index in Table 5. The proposed model ranks second only to ResUNet50 [41] by achieving Dice Scores of 0.9553 and Jaccard Index values of 0.9151. Proposed model produces segmentation results that perform nearly as well as ResUNet50 while probably needing less processing power or exhibiting higher operational speeds. These segmentation models (U-Net

765

Volume 38 No. 2s, 2025

ISSN: 1311-1728 (printed version); ISSN: 1314-8060 (on-line version)

with Attention [32], QuickTumorNet [37]) give unsatisfactory results with markedly reduced Dice scores. The proposed model demonstrates strong performance across both tumor detection and analysis roles making it a preferred selection for automated medical image analysis.

5. Conclusion and Future Scope

In this study, an improved framework for segmenting brain tumour was put forward using an optimised skip-connected ResNet-18 encoder-decoder system based on Dice loss. Through the combination of the powerful feature extraction of ResNet-18, combined with the spatial detail recovery refinement of the skip connections, the model showed an increase in accuracy to segment complex tumor areas when compared to conventional encoder-decoder models. The Dice loss developed for highly imbalanced data is the final factor that enhanced the segmentation performance by focusing on overlap of the true and predicted tumor areas. Experimental outcomes reveal that the suggested method is efficient enough in balancing out the computational efficiency and the precision of segmentation to be accommodated in clinical applications. The proposed model has attained an accuracy of 0.87%, precision of 46.99%, and F1-score and Dice coefficient of 28.27%, a Jaccard index of 44.98% and the loss in recall is minimal, around 0.84 % comparing to U-Net. This demonstrates how the precision and the degree of segmentation of the proposed model are the bettered from such results.

The future development of the improved brain tumor segmentation model has several fundamental developments. First of all, the investigation of further architectures such as ResNet-50 or the use of transformer-based models might increase the accuracy of segmentation due to the ability to represent more complex features. Developing the approach into multi-class segmentation across various tumor subregions and incorporating attention is another way to improve focusing on important parts by the model. Also, it would be possible to migrate from 2D to 3D segmentation by means of volumetric data in order to provide richer contextual information. The use of post-processing methods like Conditional Random Fields (CRFs) and transfer learning for cross-modality adaptation would improve the robustness of the model. Lastly, optimizing the model for real time deployment on edge devices would allow for immediate on-site clinical decision making, faster diagnoses and treatments rating.

References

- [1] Peddinti, A. Sravanthi, Suman Maloji, and Kasiprasad Manepalli. "Evolution in diagnosis and detection of brain tumor–review." Journal of Physics: Conference Series. Vol. 2115. No. 1. IOP Publishing, 2021.
- [2] Solanki, Shubhangi, et al. "Brain tumor detection and classification using intelligence techniques: an overview." IEEE Access 11 (2023): 12870-12886.
- [3] Anantharajan, Shenbagarajan, Shenbagalakshmi Gunasekaran, and Thavasi Subramanian. "MRI brain tumor detection using deep learning and machine learning approaches." Measurement: Sensors 31 (2024): 101026.

Volume 38 No. 2s, 2025

ISSN: 1311-1728 (printed version); ISSN: 1314-8060 (on-line version)

- [4] Xu, Wanni, You-Lei Fu, and Dongmei Zhu. "ResNet and its application to medical image processing: Research progress and challenges." Computer Methods and Programs in Biomedicine 240 (2023): 107660.
- [5] Pandey, Gaurav Kumar, and Sumit Srivastava. "ResNet-18 comparative analysis of various activation functions for image classification." 2023 International Conference on Inventive Computation Technologies (ICICT). IEEE, 2023.
- [6] Venkatraman, Shravan. "Leveraging SeNet and ResNet Synergy within an Encoder-Decoder Architecture for Glioma Detection." arXiv preprint arXiv:2409.00804 (2024).
- [7] Zhang, Wenbo, et al. "ME-Net: multi-encoder net framework for brain tumor segmentation." International Journal of Imaging Systems and Technology 31.4 (2021): 1834-1848.
- [8] Qamar, Saqib, Parvez Ahmad, and Linlin Shen. "HI-Net: Hyperdense Inception 3 D UNet for Brain Tumor Segmentation." Brainlesion: Glioma, Multiple Sclerosis, Stroke and Traumatic Brain Injuries: 6th International Workshop, BrainLes 2020, Held in Conjunction with MICCAI 2020, Lima, Peru, October 4, 2020, Revised Selected Papers, Part II 6. Springer International Publishing, 2021.
- [9] Huang, D., Wang, M., Zhang, L. et al. Learning rich features with hybrid loss for brain tumor segmentation. BMC Med Inform Decis Mak 21 (Suppl 2), 63 (2021). https://doi.org/10.1186/s12911-021-01431-y
- [10] Wang, G., Li, W., Aertsen, M., Deprest, J., Ourselin, S., & Vercauteren, T. (2018). Automatic Brain Tumor Segmentation Using Cascaded Anisotropic Convolutional Neural Networks. In BrainLes 2018: Brain Lesion Workshop, MICCAI (pp. 178–190). Springer. https://arxiv.org/abs/1712.09093
- [11] Tie, Juhong & Peng, Hui & Zhou, Jiliu. (2021). MRI Brain Tumor Segmentation Using 3D U-Net with Dense Encoder Blocks and Residual Decoder Blocks. Computer Modeling in Engineering & Sciences. 128. 427-445. 10.32604/cmes.2021.014107.
- [12] Aboussaleh, I.; Riffi, J.; Fazazy, K.E.; Mahraz, M.A.; Tairi, H. Efficient U-Net Architecture with Multiple Encoders and Attention Mechanism Decoders for Brain Tumor Segmentation. Diagnostics 2023, 13, 872. https://doi.org/10.3390/diagnostics13050872.
- [13] J. Zhang, X. Shen, T. Zhuo, and H. Zhou, "Brain Tumor Segmentation Based on Refined Fully Convolutional Neural Networks with A Hierarchical Dice Loss," arXiv.org, Dec. 25, 2017. https://arxiv.org/abs/1712.09093.
- [14] Yang, Lijuan, et al. "MUNet: a novel framework for accurate brain tumor segmentation combining UNet and mamba networks." Frontiers in Computational Neuroscience 19 (2025): 1513059.
- [15] Akshya Kumar Sahoo, Priyadarsan Parida, K. Muralibabu, Sonali Dash, Efficient simultaneous segmentation and classification of brain tumors from MRI scans using deep learning, Biocybernetics and Biomedical Engineering, Volume 43, Issue 3, 2023, Pages 616-633, ISSN 0208-5216, https://doi.org/10.1016/j.bbe.2023.08.003.

Volume 38 No. 2s, 2025

ISSN: 1311-1728 (printed version); ISSN: 1314-8060 (on-line version)

- [16] Shoushtari, Fereshteh Khodadadi, Sedigheh Sina, and Azimeh NV Dehkordi. "Automatic segmentation of glioblastoma multiform brain tumor in MRI images: Using Deeplabv3+ with pre-trained Resnet18 weights." Physica Medica 100 (2022): 51-63.
- [17] Khan, Md Kamrul Hasan, et al. "Machine learning and deep learning for brain tumor MRI image segmentation." Experimental Biology and Medicine 248.21 (2023): 1974-1992.
- [18] Kakarwal, Sangeeta, and Pradip Paithane. "Automatic pancreas segmentation using ResNet-18 deep learning approach." System research and information technologies 2 (2022): 104-116.
- [19] Francis, S. B., & Verma, J. P. (2025). Deep CNN ResNet-18 based model with attention and transfer learning for Alzheimer's disease detection. Frontiers in Neuroinformatics, 18. https://doi.org/10.3389/fninf.2024.1507217.
- [20] Zhang, Yue, et al. "Rethinking the dice loss for deep learning lesion segmentation in medical images." Journal of Shanghai Jiaotong University (Science) 26 (2021): 93-102.
- [21] K. He, X. Zhang, S. Ren and J. Sun, "Deep Residual Learning for Image Recognition," 2016 IEEE Conference on Computer Vision and Pattern Recognition (CVPR), Las Vegas, NV, USA, 2016, pp. 770-778, doi: 10.1109/CVPR.2016.90.
- [22] Goodfellow, I., Bengio, Y., & Courville, A. (2016). Deep Learning. MIT Press.
- [23] Bartz, E., Bartz-Beielstein, T., Zaefferer, M., & Mersmann, O. (2023). Hyperparameter Tuning for Machine and Deep Learning with R. https://doi.org/10.1007/978-981-19-5170-1.
- [24] Figshare Brain Tumor Dataset. Accessed: May 02, 2025. [Online]. Available: https://www.kaggle.com/datasets/ashkhagan/figshare-braintumor-dataset.
- [25] J. Cheng, W. Huang, S. Cao, R. Yang, W. Yang, Z. Yun, Z. Wang, and Q. Feng, "Enhanced performance of brain tumor classification via tumor region augmentation and partition," PLoS ONE, vol. 10, no. 10, Oct. 2015, Art. no. e0140381, doi: 10.1371/journal.pone.0140381.
- [26] K. M. Ting, "Confusion matrix," in Encyclopedia of Machine Learning, C. Sammut and G. I. Webb, Eds. Boston, MA, USA: Springer, 2010, p. 209, doi: 10.1007/978-0-387-30164-8_157.
- [27] Bertels, Jeroen, et al. "Optimizing the dice score and jaccard index for medical image segmentation: Theory and practice." Medical Image Computing and Computer Assisted Intervention–MICCAI 2019: 22nd International Conference, Shenzhen, China, October 13–17, 2019, Proceedings, Part II 22. Springer International Publishing, 2019.
- [28] Ilani, M. A., Shi, D., & Banad, Y. M. (2025). T1-weighted MRI-based brain tumor classification using hybrid deep learning models. Scientific Reports, 15(1). https://doi.org/10.1038/s41598-025-92020-w.
- [29] Shah, H. A., Saeed, F., Yun, S., Park, J., Paul, A., & Kang, J. (2022). A robust approach for brain tumor detection in magnetic resonance images using finetuned EfficientNet. IEEE Access, 10, 65426–65438. https://doi.org/10.1109/access.2022.3184113.

Volume 38 No. 2s, 2025

ISSN: 1311-1728 (printed version); ISSN: 1314-8060 (on-line version)

- [30] Mostafa, A. M., Zakariah, M., & Aldakheel, E. A. (2023). Brain tumor segmentation using deep learning on MRI images. Diagnostics, 13(9), 1562. https://doi.org/10.3390/diagnostics13091562.
- [31] F. J. D. Pernas, M. Martínez-Zarzuela, M. Antón-Rodríguez, and D. González-Ortega, "A deep learning approach for brain tumor classification and segmentation using a multiscale convolutional neural network," Healthcare, vol. 9, no. 2, p. 153, Feb. 2021.
- [32] B. V. Isunuri and J. Kakarla, "Fast brain tumour segmentation using optimized U-Net and adaptive thresholding," Automatika, vol. 61, no. 3, pp. 352–360, May 2020.
- [33] S. Tripathi, A. Verma, and N. Sharma, "Automatic segmentation of brain tumour in MR images using an enhanced deep learning approach," Comput. Methods Biomechanics Biomed. Eng., Imag. Visualizat., vol. 9, no. 2, pp. 121–130, Sep. 2020.
- [34] W. Huang and J. Wang, "Automatic segmentation of brain tumors based on DFP-UNet," in Proc. IEEE 6th Inf. Technol. Mechatronics Eng. Conf. (ITOEC), vol. 6, Mar. 2022, pp. 1304–1307.
- [35] K. Sahoo, P. Parida, K. Muralibabu, and S. Dash, "Efficient simultaneous segmentation and classification of brain tumors from MRI scans using deep learning," Biocybernetics Biomed. Eng., vol. 43, no. 3, pp. 616–633, Jul. 2023.
- [36] Ingle, M. M. Roja, M. Sankhe, and D. Patkar, "Efficient segmentation and classification of the tumor using improved encoder—decoder architecture in brain MRI images," Int. J. Electr. Comput. Eng. Syst., vol. 13, no. 8, pp. 643–651, Nov. 2022.
- [37] S. B. Kumar, R. Panda, and S. Agrawal, "Brain magnetic resonance image tumor detection and segmentation using edgeless active contour," in Proc. 11th Int. Conf. Comput., Commun. Netw. Technol. (ICCCNT), Jul. 2020, pp. 1–7.
- [38] Öksüz, O. Urhan, and M. K. Güllü, "A lightweight deep model for brain tumor segmentation," in Proc. 29th Signal Process. Commun. Appl. Conf. (SIU), Jun. 2021, pp. 1–4.
- [39] Z. Sobhaninia, S. Rezaei, N. Karimi, A. Emami, and S. Samavi, "Brain tumor segmentation by cascaded deep neural networks using multiple image scales," in Proc. 28th Iranian Conf. Electr. Eng. (ICEE), Aug. 2020, pp. 1–4.
- [40] Rehman, S. Naz, U. Naseem, I. Razzak, and I. A. Hameed, "Deep auto encoder–decoder framework for semantic segmentation of brain Tumor," Aust. J. Intell. Inf. Process. Syst., vol. 15, pp. 53–60, Jan. 2019.
- [41] Saifullah, S., Dreżewski, R., Yudhana, A., & Suryotomo, A. P. (2025). Automatic Brain Tumor Segmentation: Advancing U-Net with ResNet50 Encoder for Precise Medical Image Analysis. IEEE Access, 1. https://doi.org/10.1109/access.2025.3547430.